Lead recovery from $PbZrO_3$ using wet ball-mill technique and hydrothermal synthesis of α-zirconium phosphate from wastewater for resource recovery

Masahiro Kamiya, Ryo Sasai, Hideaki Itoh *

EcoTopia Science Institute, Nagoya University, Furo-cho, Chikusa-ku, Nagoya 464-8603, Japan

Abstract

Lead recovery from lead zirconate ($PbZrO_3$) ceramics was investigated using a wet ball-mill treatment in H_2SO_4 aqueous solution. Subsequently crystalline α-zirconium phosphate (α-$Zr(HPO_4)_2 \cdot H_2O$) was synthesized using a hydrothermal technique in order for the resource recovery of zirconium in the wastewater after the wet ball-mill treatment. A wet ball-mill treatment in 4.5 M H_2SO_4 aqueous solution for 24 h was capable of converting more than 99.9% of the Pb initially included in the $PbZrO_3$ to solid state $PbSO_4$ with a purity of 98%. On the other hand, the Zr in the $PbZrO_3$ was dissolved into the acidic solution during the treatment. The Pb and Zr metal elements coexisting in $PbZrO_3$ were successfully separated by the wet ball-mill technique. Then, resource recovery of zirconium in the wastewater was examined. Crystalline α-$Zr(HPO_4)_2 \cdot H_2O$ was synthesized by hydrothermal treatments in 3.1–12.5 M H_3PO_4 aqueous solutions at temperatures of 120–240 °C for a duration of 70 h. The hydrothermally prepared powders were characterized by X-ray diffraction (XRD) and scanning electron microscopy (SEM), and then they were also evaluated in terms of cation exchange capacity (CEC) measurement and thermogravimetric (TG) analysis.
© 2005 Elsevier B.V. All rights reserved.

Keywords: Lead recovery; Ball-mill; Zirconium phosphate; Hydrothermal synthesis

1. Introduction

In recent years, serious attempts to minimize the use of lead and substitute other lead-free materials in place of lead-based materials in products have been made, because lead, when contained in the human body, is a hazardous heavy metal. However, a large number of lead-containing products, such as lead accumulators, lead glass, solder and lead-based electronic devices, have been produced and consumed as yet. Some lead-containing wastes from industries and households have been landfilled without recovering lead in the products or recycling it as a resource. Specifically, lead-based electronic materials are widely used in electronic devices, and lead discharge after the usage seems to be inevitable even in the future due to their superior properties [1–3]. It is important to develop the lead-condensation and separation technology as a recyclable form from other metals, which are included in lead-based electronic ceramics and the electronic devices, as well as the separation technology of lead-containing parts in products. We reported that a wet ball-mill treatment in H_2SO_4 aqueous solution at room temperature was applicable to preferable recovery of lead from lead-based electronic ceramics such as $Pb(Zr_{0.52}Ti_{0.48})O_3$ and $(Pb_{0.9}La_{0.1})(Zr_{0.52}Ti_{0.48})O_3$ [4,5]. Both of the dissolution of PZT and PLZT into the H_2SO_4 solution and the formation of water-insoluble $PbSO_4$ precipitate were efficiently progressed by the pulverization and mechanical activation of the powder during the ball-milling. Through this treatment, more than 99.9% of lead originally included in these ceramics was successfully converted into high purity $PbSO_4$ [4]. However, other metal components such as zirconium and titanium still remained in the wastewater after the treatment.

Layered tetravalent metal hydrogen phosphates with the composition $M(HPO_4)_2 \cdot H_2O$ (M = Zr, Ti, etc.) have attracted much attention because of their excellent properties as cation exchangers [6–12], acid catalyst [13–15] and host material for intercalating polar molecules [16]. The crystalline α-$Zr(HPO_4)_2 \cdot H_2O$ was mainly prepared using a pure starting material through two different routs. The first is a reflux method, in which gelatinous precursor is firstly prepared and then crystallized in a hot

---

* Corresponding author. Tel.: +81 52 789 5854; fax: +81 52 789 5853.
E-mail address: hitoh@esi.nagoya-u.ac.jp (H. Itoh).

H_3PO_4 aqueous solution [6,8]. The other method is a precipitation method using HF solution, where the gelatinous precursor is dissolved into a HF solution and then the solution is slowly evaporated in order to deposit the phosphate [17]. The phosphate obtained from the HF solution is highly crystallized and is larger grained in comparison with that prepared by reflux method.

In the present research, lead zirconate ($PbZrO_3$), which was expected to show the similar behavior to PZT and PLZT, was treated by the wet ball-mill technique in H_2SO_4 aqueous solution to recover lead separately into a solid state of $PbSO_4$. Subsequently, α-zirconium phosphate (α-$Zr(HPO_4)_2 \cdot H_2O$) was hydrothermally synthesized in order for the resource recovery of zirconium in the wastewater. In addition, some properties of the hydrothermally prepared phosphates such as cation exchange capacity (CEC) and its thermal behavior were evaluated in comparison to those of the reported phosphates prepared from pure materials.

2. Experimental procedure

2.1. Wet ball-mill treatment of PbZrO₃ and hydrothermal synthesis of α-Zr(HPO₄)₂·H₂O

Commercially available sintered $PbZrO_3$ (Kojundo Chemical Lab Co., Ltd., Japan) was used as a model material for the wet ball-mill treatment. First, a sintered compact was precrushed using an agate mortar and pestle. The powdery sample (approximately 5.5 mmol) was charged into a polypropylene container with a volumetric capacity of 50 ml together with ZrO_2 balls (ϕ 5 mm, weight ratio of the sample/ZrO_2 = 1/50), and then 4 ml of 4.5 M H_2SO_4 was poured into the container. The container was rotated with a constant speed of 300 rpm for durations of 4–48 h. After the ball-mill treatment, samples and balls were treated with sonication in 100 ml of 0.5 M H_2SO_4 to disperse the solids attached on the balls into the solution. Then, the solid residues and solution were separated by filtration under reduced pressure with a membrane filter (<0.45 μm).

Zirconium ions in the filtrate were used as zirconium resource for the hydrothermal synthesis of crystalline α-$Zr(HPO_4)_2 \cdot H_2O$. First, 0.3 M H_3PO_4 solution was slowly added into the wastewater while vigorously stirring in order to obtain amorphous zirconium phosphate. After stirring for 1 h, the white precipitate was collected in the filtration process, washed with deionized water and dried at 110 °C for 24 h. Amorphous phosphate was crystallized using a hydrothermal technique. Approximately 0.3 g of the dried sample and 30 ml of H_3PO_4 aqueous solution (3.1–12.5 M) were enclosed into an autoclave lined with Teflon with a volumetric capacity of 50 ml. The autoclave was heated in the temperature range of 120–240 °C for 70 h. After hydrothermal treatment, the solid residues were collected through filtration, washed with deionized water and finally dried at 50 °C for 24 h.

2.2. Characterization

The raw material and the treated samples were identified by powder X-ray diffraction (XRD; RINT2500H, Rigaku).

Microstructure observation was performed by a scanning electron microscope (SEM; JSM-6330F, JEOL) equipped with an energy dispersive spectrometer (EDS; JED-2140, JEOL). Quantitative analyses of Pb and Zr dissolved in the filtrate were performed by inductively coupled plasma atomic-emission spectroscopy (ICP-AES; 3300DV, Perkin-Elmer, Japan). Specific surface areas were calculated from the amount of N_2 gas adsorbed at the temperature of liquid nitrogen by one-point BET method (MS-21, Quantachrome) in He–30%N_2 (N_2 partial pressure, P/P_0 = 0.30). Cation exchange capacity (CEC) of the prepared phosphate was measured through a titration curve, which was acquired as follows. First, 0.1 g of the phosphate was equilibrated with the 50 mL of 0.1 M NaCl with stirring and then the pH of the suspension was recorded using a digital pH meter (HORIBA, D-21). Next, a constant volume of 0.01 M NaOH solution was poured using a micropipette into the solution during the stirring process, and the pH was recorded when the pH drift was less than 0.01/min. The titration was continuously carried out until the final pH of the solution reached 8–9. All of the titration operations were conducted in a thermostatic bath regulated at 27 °C. High-temperature XRD patterns were acquired in the temperature range from room temperature to 1000 °C in air holding for 5 min at each temperature. TG and DTA was carried out under flowing O_2–N_2 (O_2; 20 ml/min, N_2; 80 ml/min) at the heating rate of 10 K/min in the temperature range from room temperature to 1000 °C.

3. Results and discussion

3.1. Recovery of lead from PbZrO₃ using a wet ball-mill treatment

Fig. 1 shows XRD profiles of (a) $PbZrO_3$, and the specimens after a wet ball-mill treatment with 4.5 M H_2SO_4 aqueous solution for (b) 5 and (c) 24 h. XRD profile in Fig. 1(a) is the $PbZrO_3$ model material used in the present study. The ball-milled sample for 5 h in Fig. 1(b) was composed of $PbZrO_3$ and orthorhombic $PbSO_4$. The $PbZrO_3$ peak intensity gradually decreased with increasing treatment time. XRD profiles in Fig. 1(c) showed
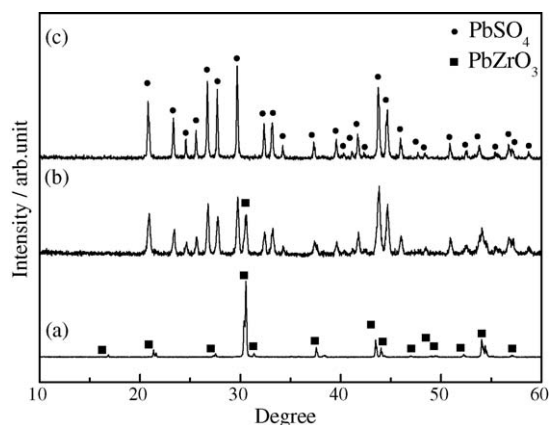

Fig. 1. XRD profiles of the (a) $PbZrO_3$ model material and the specimens after a wet ball-mill treatment with 4.5 M H_2SO_4 aqueous solution for (b) 5 and (c) 24 h.

Table 1
Purities of the recovered $PbSO_4$ calculated from ICP results

Time (h)	Initial contents (mg)		Dissolution (%)		Converted mass (mg)		$PbSO_4$ (mass%)
	Pb	Zr	Pb	Zr	$PbSO_4$	ZrO_2	
5	1136.7	500.4	0.07	26.3			
24	1137.1	500.6	0.06	96.9	1663.2	20.1	98.8
48	1137.2	500.7	0.06	96.5	1663.2	22.3	98.6

that the milled samples were mainly composed of $PbSO_4$ phase without $PbZrO_3$ phase. The analysis of the filtrate by ICP-AES in Table 1 showed that the dissolution of Zr gradually increased and reached around 97%, while the dissolution of Pb ion into the filtrate was less than 0.07% under the whole treatments, which indicates that most of Pb exists in the solid phase, i.e., $PbZrO_3$ or $PbSO_4$ phase. More than 99.9% Pb was recovered as solid state of $PbSO_4$ by the ball-mill treatment with 4.5 M H_2SO_4 solution for 24 h. The effect of the wet ball-mill treatment on the decomposition of $PbZrO_3$ is briefly stated here. $PbZrO_3$ is pulverized into a fine powder, and the particles are well dispersed in the solution during the wet ball-mill treatment. The mechanically activated $PbZrO_3$ particle easily undergoes an acidic solvent attack and begins to dissolve into the acidic solution. The dissolved lead component readily precipitated into a solid state of $PbSO_4$. The rotation of the reaction container and the collision between the ball and specimen during the treatment are effective to automatically remove the $PbSO_4$ adhered to the specimen surface and to continuously expose the fresh specimen surfaces. As a result, treatment efficiency for the conversion of $PbZrO_3$ to $PbSO_4$ was enhanced using a combination of mechanical work and chemical reaction. The purity of the recovered $PbSO_4$ after ball-mill treatments for durations of 24 and 48 h is also listed in Table 1. Purity of $PbSO_4$ in the solid residue was estimated from a comparison between the initial contents and dissolution amounts of Pb and Zr, taking into account that both elements exist in the residue as a form of $PbSO_4$ and ZrO_2. The purity of $PbSO_4$ was calculated around 98.6–98.8%. A similar value was also confirmed by a complete analysis of the solid residue using ICP-AES as 66.9 mass% of Pb and 0.8 mass% of Zr, which suggested 98 mass% of $PbSO_4$.

3.2. Hydrothermal synthesis of α-$Zr(HPO_4)_2 \cdot H_2O$ for resource recovery in wastewater

First, an aqueous solution of H_3PO_4 was added into wastewater discharged after the wet ball-mill treatment to collect amorphous zirconium phosphate, which was used for the subsequent hydrothermal crystallization. The amount of added H_3PO_4 aqueous solution was optimized to reclaim a larger amount of zirconium resource from the wastewater. Fig. 2 shows the variation of residual metal ion ratios in the wastewater after H_3PO_4 addition. The residual Zr ion ratio markedly decreased with an increasing H_3PO_4 amount up to 3.2 in H_3PO_4/Zr molar ratio, at which more than 99% of Zr precipitated as amorphous zirconium phosphate. Further the H_3PO_4 addition was not effective to precipitate zirconium ions. On the other hand, no serious decrease in the residual Pb ion ratio could be observed, which indicated that most of

the Pb still remained in the wastewater. The small amount of Pb decrease was probably caused by co-precipitation or cation exchange ability of amorphous zirconium phosphate. As a result, the suitable H_3PO_4 amount was determined to be 3.2, at which a relatively large amount of zirconium could be reclaimed by a smaller addition of H_3PO_4.

The amorphous zirconium phosphate was crystallized by hydrothermal treatments in 3.1–12.5 M H_3PO_4 aqueous solutions at 120–240 °C. The zirconium species initially deposited were in an amorphous form, and the deposits gradually crystallized in α-$Zr(HPO_4)_2 \cdot H_2O$ with increasing hydrothermally treated time. Fig. 3 shows XRD patterns of solid residues as-prepared by hydrothermal treatments in 6.2 M H_3PO_4 for 70 h at varied temperatures. The solid residues were mainly composed
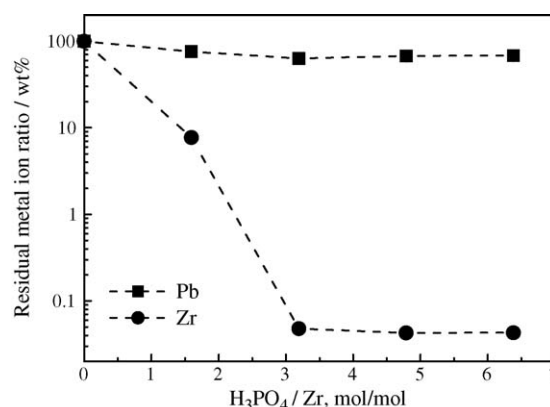

Fig. 2. Variation of the residual metal ion ratios for (■) Pb and (●) Zr in wastewater after wet ball-mill treatment for 24 h with varied H_3PO_4 addition.
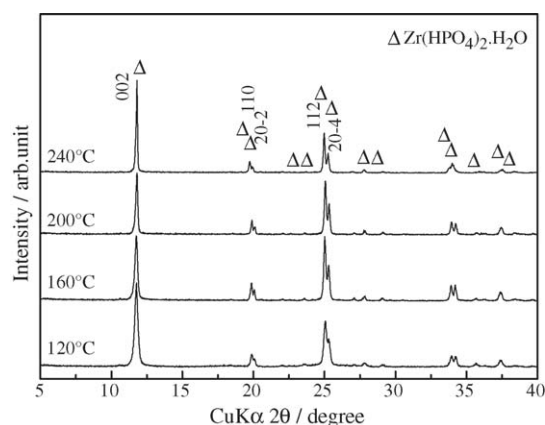

Fig. 3. XRD profiles of the solid precipitates obtained by hydrothermal treatment in 6.2 M H_3PO_4 for a duration of 70 h at various temperatures.
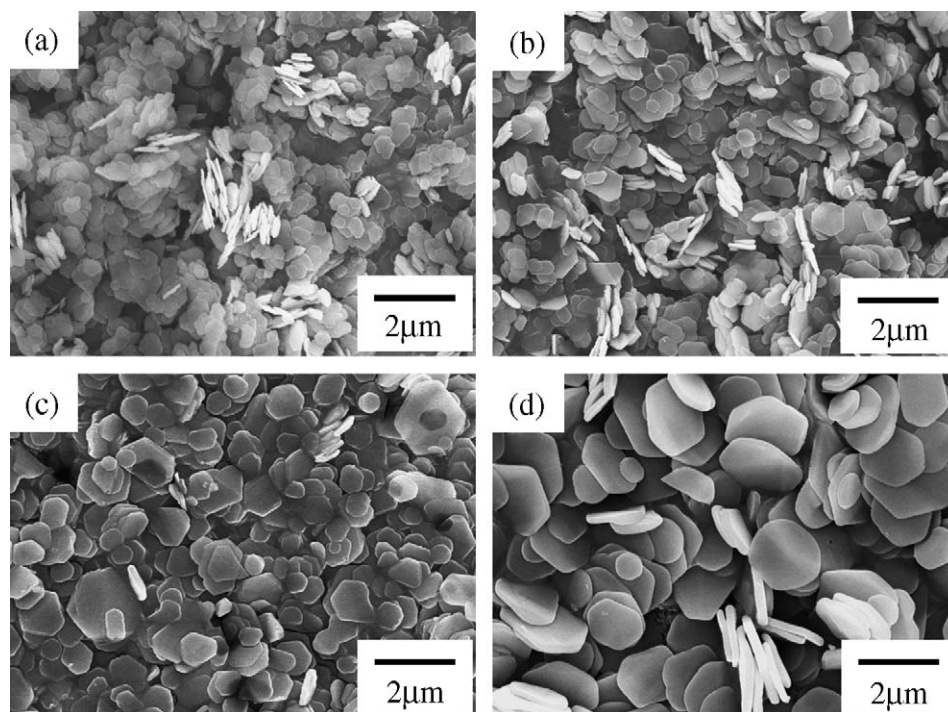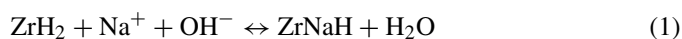
Fig. 4. SEM micrographs of α-Zr(HPO$_4$)$_2$·H$_2$O prepared by hydrothermal treatment in 6.2 M H$_3$PO$_4$ at various temperatures. The processing temperatures are (a) 120, (b) 160, (c) 200 and (d) 240 °C, respectively.

of monoclinic α-Zr(HPO$_4$)$_2$·H$_2$O phase. For the treatment in the solvent of the lowest concentration of 3.1 M at the lowest temperature of 120 °C, the hydrothermal condition was insufficient to crystallize amorphous phase in α-Zr(HPO$_4$)$_2$·H$_2$O phase since only the weak and broad peaks could be observed in the XRD pattern. While with increasing treatment temperature and H$_3$PO$_4$ concentration, the obtained phosphate showed higher crystallinity and larger crystallites since the diffraction peaks sharpened and FWHM (full width of half maximum) became smaller.

Fig. 4 shows typical SEM micrographs of solid residues as-prepared after hydrothermal treatments in 6.2 M H$_3$PO$_4$ solution for various temperatures. All of the solid residues consisted of fine plate-like particles. As the treatment temperature increased from 120 to 240 °C, the particle size increased from nearly sub-micron to 4 μm and the thickness of the particles also increased. Hydrothermal treatments under higher temperature and higher H$_3$PO$_4$ concentration lead to recrystallization and grain growth of the deposits that resulted in the formation of a thick plate-like phosphate particle.

CEC of α-Zr(HPO$_4$)$_2$·H$_2$O prepared by hydrothermal treatment under various conditions can be estimated from titration curves, which are shown in Fig. 5. The titration curves of the phosphates prepared by hydrothermal treatments at a fixed temperature of 200 °C in H$_3$PO$_4$ with varied concentrations in Fig. 5(a) drew a similar curve for each other. The curves consisted of two plateaus, each plateau corresponding to the exchange of 1 mol of a hydrogen ion with a sodium ion per mol of phosphate, because the crystalline α-Zr(HPO$_4$)$_2$·H$_2$O has two types of acid sites with a remarkably different acid strength from each another, in which the weak acid site is P–OH

group with strong interaction with crystal water and the strong acid site is free P–OH [15]. Furthermore, the fully crystallized α-Zr(HPO$_4$)$_2$·H$_2$O exhibits definite zero slope in titration curve since one solid-solution phase is formed. The curves also exhibit two inflections in the pH range around 4–5 and 7–8, which indicate the first and second end points of the following reactions,

$$ZrH_2 + Na^+ + OH^- \leftrightarrow ZrNaH + H_2O \tag{1}$$

and

$$ZrNaH + Na^+ + OH^- \leftrightarrow ZrNa_2 + H_2O, \tag{2}$$
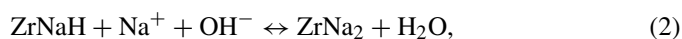
respectively. The first and the second end points occur at approximately 3.2 and 6.5 meq/g, respectively. CEC of α-Zr(HPO$_4$)$_2$·H$_2$O prepared in this study was 6.5 meq/g, nearly corresponding to the theoretical CEC of 6.6 meq/g. Similar curves could be acquired in the phosphates prepared by hydrothermal treatments at 240 °C.

In contrary to the titration curves of the phosphates hydrothermally prepared at 200 °C in Fig. 5(a), significant differences were observed in the titration curves of the phosphates after hydrothermal treatment in 6.2 M H$_3$PO$_4$ aqueous solution at various temperatures, as shown in Fig. 5(b). The difference would come from the inconsistency in the crystallinity of α-Zr(HPO$_4$)$_2$·H$_2$O due to the formation of one or more solid-solution phases with a variable composition in the α-Zr(HPO$_4$)$_2$·H$_2$O [8], which cause the non-zero slope in the titration curve. The CEC tended to decrease along with the decreasing treatment temperature, which seemed to own small particle size and the existence of amorphous phases. Pb ion was
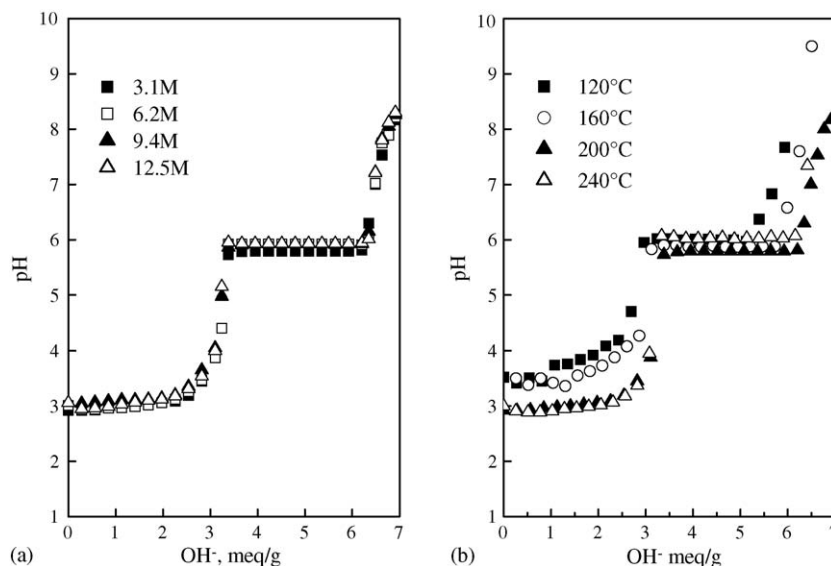
Fig. 5. Titration curves of α-Zr(HPO$_4$)$_2$·H$_2$O prepared by hydrothermal treatments: (a) in various H$_3$PO$_4$ concentrations at 200 °C and (b) in 6.2 M H$_3$PO$_4$ at various temperatures.

not detected by ICP-AES analysis of the solution in the pH ranges of 3–8 during the titration.

The thermal behavior of α-Zr(HPO$_4$)$_2$·H$_2$O was examined by high-temperature XRD and TG–DTA. Typical high-temperature XRD patterns at various temperatures are shown in Fig. 6. The thermal transformation sequence was mostly the same between the samples when the calcination temperature was lower than 600 °C, as reported thermal transformation [18]. By heating up to 200 °C, anhydration of crystal water occurred, which resulted in the formation of Zr(HPO$_4$)$_2$ (η phase) through Zr(HPO$_4$)$_2$ (ξ phase). Further heating from 600 up to 1000 °C lead to the distinctly difference in thermal transformations among the samples.

Upon increasing the heating temperature, the diffraction peaks of η phase were gradually weakened and completely disappeared at 700 °C on the sample prepared at 120 °C in 12.5 M H$_3$PO$_4$, the peaks of η phase still remained in the sample prepared at 200 °C in 6.4 M H$_3$PO$_4$. When the calcination temperature was 900 °C, sharp peaks of cubic ZrP$_2$O$_7$ phase appeared for the sample prepared at 120 °C, but the ZrP$_2$O$_7$ phase was not formed for the sample prepared at 200 °C. The difference in the crystallization behavior of ZrP$_2$O$_7$ most likely came from the differences in the grain size [19], as seen in Fig. 4.

Typical TG–DTA curves of α-Zr(HPO$_4$)$_2$·H$_2$O are shown in Fig. 7. Weight loss attributed to desorption of the surface
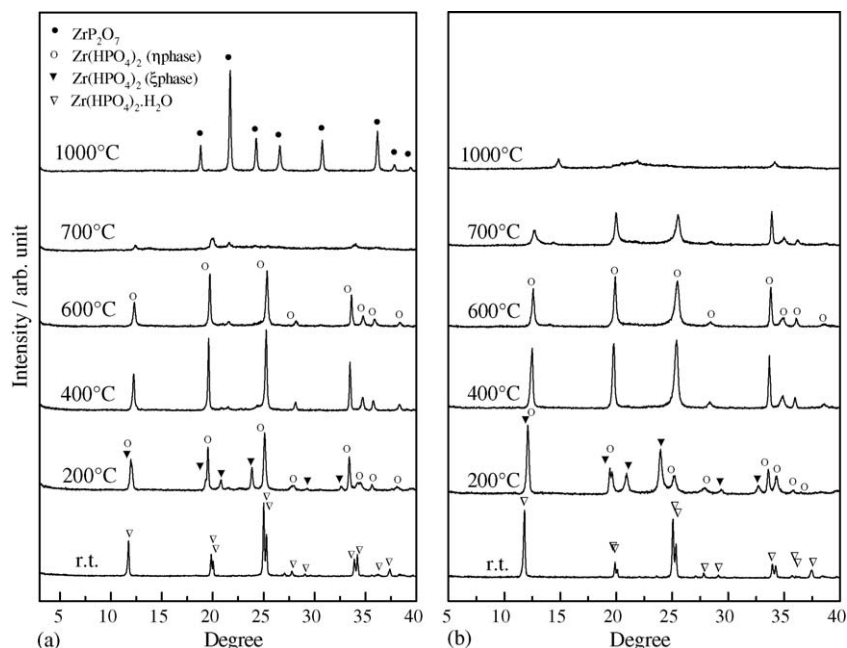

Fig. 6. High-temperature X-ray diffraction patterns of α-Zr(HPO$_4$)$_2$·H$_2$O prepared by hydrothermal treatments: (a) in 12.5 M H$_3$PO$_4$ at 120 °C and (b) in 6.2 M H$_3$PO$_4$ at 200 °C.
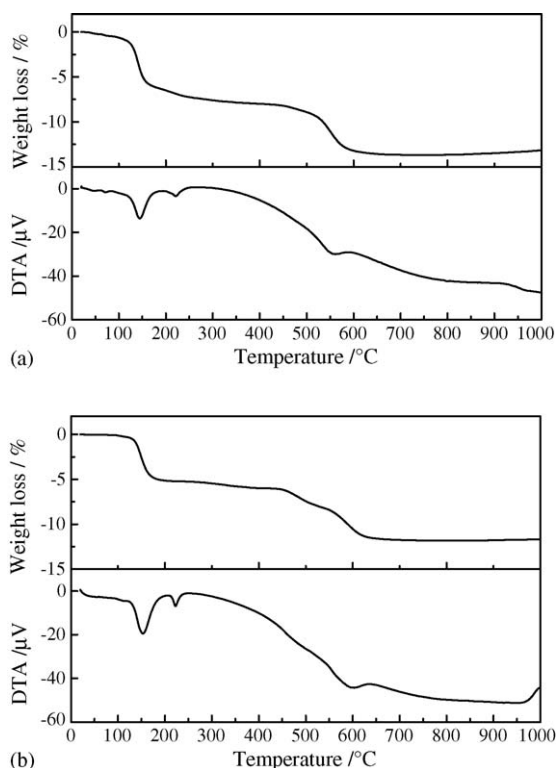
Fig. 7. TG–DTA curves of α-Zr(HPO$_4$)$_2$·H$_2$O prepared by hydrothermal treatments: (a) in 12.5 M H$_3$PO$_4$ at 120 °C and (b) in 6.2 M H$_3$PO$_4$ at 200 °C.

adsorbed water which started below 100 °C and subsequently TG–DTA curves showed broad endothermic peak with weight loss at around 150 °C in both samples. Generally, the endothermic peak is ascribed to the formation of the anhydrous phase of ξ-ZrP according to the reaction [18,19]

$$\alpha\text{-Zr(HPO}_4)_2 \cdot \text{H}_2\text{O} \rightarrow \xi\text{-Zr(HPO}_4)_2 + \text{H}_2\text{O}. \quad (3)$$

The anhydration of crystal water accompanied the change of interlayer distance from 7.56 of α phase to 7.41 Å of ξ phase. The amount of the weight loss of the sample prepared at 120 °C was also larger than that of the prepared sample of 200 °C. The second sharp endothermic peak without weight loss is then observed at 220 °C associated with enantiotropic change of phase described as [18]
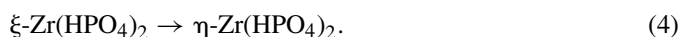
$$\xi\text{-Zr(HPO}_4)_2 \rightarrow \eta\text{-Zr(HPO}_4)_2. \quad (4)$$

Further heating lead to the formation of ZrP$_2$O$_7$ with the loss of constituent water,

$$\eta\text{-Zr(HPO}_4)_2 \rightarrow \text{ZrP}_2\text{O}_7 + \text{H}_2\text{O}. \quad (5)$$
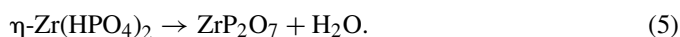
All phases formed through the transformation from α-Zr(HPO$_4$)$_2$·H$_2$O to ZrP$_2$O$_7$ was confirmed by high-temperature XRD as shown in Fig. 6. Theoretical weight loss from α-Zr(HPO$_4$)$_2$·H$_2$O to ZrP$_2$O$_7$ was calculated at 11.96%. The experimental weight loss of α-Zr(HPO$_4$)$_2$·H$_2$O prepared at 200 and 120 °C were 11.8 and 13.1%, respectively.

4. Summary

We attempted to develop a non-heating lead recovering method in lead-based electronic ceramics by new mechanochemical technique. Pb and Zr contained in PbZrO$_3$ ceramics were successfully separated using a wet ball-mill treatment with a 4.5 M H$_2$SO$_4$ aqueous solution, in which Pb was reclaimed in a solid state of PbSO$_4$ and Zr was dissolved into filtrate. The purity of reclaimed PbSO$_4$ was around 98.6–98.8%. Subsequently, a useful chemical α-Zr(HPO$_4$)$_2$·H$_2$O were synthesized using a hydrothermal technique in order for the resource recovery of zirconium contained in the wastewater discharged after wet ball-mill treatments. Highly crystallized and larger grained α-Zr(HPO$_4$)$_2$·H$_2$O could be synthesized by hydrothermal treatment of H$_3$PO$_4$ aqueous solutions at 200 and 240 °C for 70 h. Cation exchange capacity measurement and thermal transformation examination revealed that the obtained α-Zr(HPO$_4$)$_2$·H$_2$O had similar properties in comparison with the prepared pure materials.

References

[1] E. Fukuchi, T. Kimura, T. Tani, T. Takeuch, Y. Saito, Effect of potassium concentration on the grain orientation in bismuth sodium potassium titanate, J. Am. Ceram. Soc. 85 (6) (2002) 1461–1465.

[2] C.F. Buhrer, Some properties of bismuth perovskites, J. Chem. Phys. 36 (1962) 798–803.

[3] R.J. Xie, Y. Akimune, K. Matsuo, T. Sugiyama, Dielectric and ferroelectric properties of tetragonal tungsten bronze Sr$_{2-x}$Ca$_x$NaNb$_5$O$_{15}$ ($x = 0.05$–0.35) ceramics, Appl. Phys. Lett. 80 (2002) 835–837.

[4] M. Kamiya, R. Sasai, H. Itoh, Recovery of lead in lead zirconate titanate ceramics by wet ball mill with acidic solution, J. Ceram. Soc. Japan 111 (2003) 806–810.

[5] M. Kamiya, R. Sasai, H. Itoh, Recovery of lead from PLZT ceramics using the wet ball-mill method, J. Ceram. Soc. Japan 111 (2003) 897–901.

[6] A. Clearfield, J.A. Styness, The preparation of crystalline zirconium phosphate and some observations on its ion exchange behavior, J. Inorg. Nucl. Chem. 26 (1964) 117–129.

[7] G. Alberti, P. Cardini-Galli, U. Costantino, T. Torracca, Crystalline insoluble salts of polybasic metals-I. Ion-exchange properties of crystalline titanium phosphate, J. Inorg. Nucl. Chem. 29 (1967) 571–578.

[8] A. Clearfield, L. Kullberg, Å. Oskarsson, On the mechanism of ion exchange in crystalline zirconium phosphates. XI. The variation in unit cell dimensions and sodium ion/hydrogen ion exchange behavior in highly crystalline α-zirconium phosphates, J. Phys. Chem. 78 (1974) 1150–1153.

[9] S. Roca, C. Airoldi, Thermodynamic data of ion exchanger on amorphous titanium (IV) phosphate, Thermochim. Acta 284 (1996) 289–297.

[10] L.M. Nunes, C. Airoldi, Some features of crystalline α-titanium hydrogenphosphate, modified sodium and n-butylammonium forms and thermodynamics of ionic exchange with K$^+$ and Ca^{2+}, Thernochim. Acta 328 (1999) 297–305.

[11] U. Costantio, L. Szirtes, E. Kuzmann, J. Megyeri, K. Lázár, Exchange of iron ions into layers of α-zirconium phosphate, Solid State Ionics 141–142 (2001) 359–364.

[12] B.B. Sahu, K. Parida, Cation exchange and sorption properties of crystalline α-titanium(IV) phosphate, J. Colloids Interface Sci. 248 (2002) 221–230.

[13] A. Clearfield, D.S. Thakur, Zirconium and titanium phosphates as catalysts: a review, Appl. Catal. 26 (1986) 1–26.

[14] S. Cheng, A. Clearfield, Acidity and catalytic properties of zirconium phosphate, Appl. Catal. 26 (1986) 91–101.

[15] T. Hattori, A. Ishiguro, Y. Murakami, Acidity of crystalline zirconium phosphate, J. Inorg. Nucl. Chem. 40 (1978) 1107–1111.

[16] H. Nakayama, A. Hayashi, T. Eguchi, N. Nakamura, M. Tsuhako, Adsorption of formaldehyde by polyamine-intercalated α-zirconium phosphate, Solid State Sci. 4 (2002) 1067–1070.

[17] G. Alberti, E. Torracca, Crystalline insoluble salts of polybasic metals-II. Synthesis of crystalline zirconium or titanium phosphate by direct precipitation, J. Inorg. Nucl. Chem. 30 (1968) 317–318.

[18] R.C.T. Slade, J.A. Knowles, D.J. Jones, J. Roziére, The isomorphous acid salts α-Zr(HPO$_4$)$_2$·H$_2$O, α-Ti(HPO$_4$)$_2$·H$_2$O and α-Zr(HAsO$_4$)$_2$·H$_2$O. Comparative thermochemistry and vibrational spectroscopy, Solid State Ionics 96 (1997) 9–19.

[19] U. Costantino, R. Vivani, V. Zima, E. Cernoskova, Thermoanalytical study, phase transitions, and dimensional changes of α-Zr(HPO$_4$)$_2$·H$_2$O large crystals, J. Solid State Chem. 132 (1997) 17–23.